ELSEVIER

European Journal of Pharmacology 382 (1999) 217–227

ejp

www.elsevier.nl/locate/ejphar

The assessment of antagonist potency under conditions of transient response kinetics

Arthur Christopoulos [a,1,3], Ann M. Parsons [a,2,3], Michael J. Lew [b], Esam E. El-Fakahany [a,*]

[a] *Departments of Neuroscience, Psychiatry and Pharmacology, Box 392, Mayo Memorial Building, University of Minnesota Medical School, Minneapolis, MN, 55455, USA*

[b] *Department of Pharmacology, University of Melbourne, Parkville, 3052, Victoria, Australia*

Received 8 April 1999; received in revised form 23 July 1999; accepted 30 July 1999

Abstract

The muscarinic acetylcholine receptor antagonists, atropine and pirenzepine, produced an apparent insurmountable antagonism of muscarinic M_1 receptor-mediated intracellular Ca^{2+} mobilization in Chinese hamster ovary (CHO) cells when tested against the agonists carbachol or xanomeline. Each antagonist caused a dextral shift of the agonist concentration–response curves with depression of the maximum response that was incomplete (i.e., saturated) and which varied with the pairs of agonist and antagonist. Equilibrium competition binding assays found no deviation from simple, reversible competitive behavior for either antagonist. The relative rates of dissociation of unlabeled atropine and pirenzepine were also assessed in radioligand kinetic studies and it was found that atropine dissociated from the receptor approximately 8-fold slower than pirenzepine. Numerical dynamic simulations suggested that the insurmountability of antagonism observed in the present study was probably a kinetic artifact related to the measurement of transient responses to a non-equilibrated agonist in the presence of a slowly dissociating antagonist. Importantly, the patterns of antagonism observed included a saturable depression of agonist maximal response, a mode of antagonism that is incompatible with the previously described phenomenon of hemi-equilibrium states. Monte Carlo simulations indicated that reasonable, semi-quantitative estimates of antagonist potency could be determined by a minor modification of standard methods, where equieffective agonist concentrations, rather than EC_{50} values, are compared in the absence and presence of antagonist. Application of the latter approach to the functional data yielded estimates of antagonist potency that were in excellent agreement with those derived from the equilibrium binding assays, thus indicating that the present method can be useful for quantifying antagonist potency under non-equilibrium conditions.

Keywords: Muscarinic receptor; Transient response; Ca^{2+} mobilization; Monte Carlo simulation; Kinetics; Antagonism; Insurmountable

1. Introduction

In recent times, much attention has been drawn to the fact that the properties of agonist affinity and efficacy are inextricably linked to such an extent that unambiguous estimates of the former property for the purpose of receptor classification are difficult to obtain (Kenakin, 1997; Colquhoun, 1998; Christopoulos and El-Fakahany, 1999). In contrast, the use of competitive, neutral, antagonists in the classification process overcomes this drawback and, as a consequence, that approach has remained the pre-eminent means for the pharmacological classification of receptor systems. A traditional hallmark of competitive antagonism in functional assays is the ability of the antagonist to produce parallel, dextral shifts of an agonist concentration–response curve with no change in the maximum agonist response. In fact, these features are often cited as the minimal requirements for presumptive evidence of the operation of a reversible, competitive mechanism (Kenakin, 1997). However, there have been a number of instances where certain antagonists appeared to satisfy the classic criteria for competitive, surmountable, antagonism in some assays but not in others, even though in each

* Corresponding author. Tel.: + 1-612-624-8432; fax: + 1-612-624-8935; e-mail: elfak001@maroon.tc.umn.edu

[1] Present address: Department of Pharmacology, University of Melbourne, Parkville, 3052, Victoria, Australia.

[2] Present address: University of Wisconsin-Stout, Biology Department, Menomonie, WI, 54751, USA.

[3] These authors contributed equally to this work.

0014-2999/99/$ - see front matter
PII: S0014-2999(99)00550-6

instance the same receptor type was studied in the same tissue. Importantly, the response being measured in most cases was one that was proximal to receptor activation. For example, El-Fakahany et al. (1988) demonstrated how the muscarinic acetylcholine receptor antagonist, pirenzepine, appeared competitive at the muscarinic M_1 receptor in assays of radioligand binding and phosphoinositide hydrolysis, but not so in functional assays measuring intracellular cGMP formation, where an apparent insurmountable antagonism was observed. Kukkonen et al. (1997; 1998) have extended these observations to the measurement of intracellular Ca^{2+} mobilization mediated either by α_2-adrenoceptors or muscarinic receptors. In fact, the phenomenon of apparent insurmountability of antagonism for competitive antagonists appears quite widespread across a range of receptor systems and assays (Paton and Waud, 1967; Kenakin and Cook, 1980; Kachur et al., 1988; Bond et al., 1989; Boselli and Kenakin, 1990; Kenakin and Boselli, 1990; Liu et al., 1992; Robertson et al., 1994; Hara et al., 1995). Although a number of potential mechanisms have been postulated in order to account for this phenomenon, a common explanation that has been proposed is one of non-equilibrium conditions operating over the short time-course of response measurement due to slow antagonist dissociation kinetics. Unfortunately, the majority of such studies to date have treated this apparent insurmountability of antagonism qualitatively as an unavoidable kinetic artifact, and no attempts have thus been made to quantify antagonist potency under these conditions. The remaining studies that have attempted to derive some form of quantitative information from the data have invariably utilized equilibrium formulations to assign ''meaningful'' values to parameters determined under non-equilibrium conditions, or have not addressed the problem as a kinetic artifact altogether.

Under conditions of rapid and transient agonist response kinetics, the equilibrium assumption, so crucial to the classical approaches describing and quantifying competitive antagonism, is inappropriate, and deviations from equilibrium behavior need to be accounted for. Unfortunately, the non-equilibrium problem is sometimes unavoidable, for example, in the measurement of real-time Ca^{2+} transients and for many other responses proximal to receptor activation that can be measured with modern technologies. It would be useful to derive at least a semi-quantitative approach that should allow for antagonist potency estimates to be determined that do not drastically deviate from their equilibrium values. Thus, the aim of the present study was to derive potency estimates at the muscarinic M_1 muscarinic acetylcholine receptor of the antagonists, atropine and pirenzepine, for their ability to inhibit agonist-mediated intracellular Ca^{2+} mobilization, which, by its nature, is a transient response. In addition, a dynamic simulation and Monte Carlo approach was used to assess the reliability of these estimates, assuming that they were obtained under non-equilibrium conditions.

2. Materials and methods

2.1. Materials

[^{3}H]*N*-methylscopolamine (84.5 Ci/mmol) was purchased from NEN Dupont (Wilmington, DE); Dulbecco's modified Eagle's medium was purchased from GIBCO (Gaithersburg, MD); geneticin and Fura 2/AM were purchased from Calbiochem (La Jolla, CA); bovine calf serum was purchased from Hyclone (Logan, UT); xanomeline tartrate was a generous gift from Lilly Research Laboratories (Indianapolis, IN). All other reagents were purchased from Sigma (St. Louis, MO).

2.2. Cell culture

Chinese hamster ovary (CHO) cells, stably expressing the human muscarinic M_1 acetylcholine receptor (provided by Dr. M. Brann, University of Vermont Medical School, Burlington, VT) were grown for 4 days at 37°C in Dulbecco's modified Eagle's medium, supplemented with 10% bovine calf serum and 50 μg/ml geneticin, in a humidified atmosphere consisting of 5% CO_2 and 95% air. Cells were used 4 days after subculture, and were harvested by trypsinization followed by centrifugation ($300 \times g$, 3 min) and re-suspension of the pellet in HEPES buffer (110 mM NaCl, 5.4 mM KCl, 1.8 mM $CaCl_2$, 1 mM $MgSO_4$, 25 mM Glucose, 50 mM HEPES, 58 mM Sucrose; pH 7.4; 340 mOsm), repeated twice.

2.3. Intracellular Ca^{2+} measurements

Muscarinic receptor-mediated changes in the levels of intracellular Ca^{2+} in response to the agonists carbachol or xanomeline were measured using the Ca^{2+}-binding dye Fura 2/AM as previously described (Wotta et al., 1998). Briefly, cells were harvested and washed in HEPES buffer, as described above. The dye was then loaded by incubation of the cells ($2–3 \times 10^7$ cells/ml HEPES buffer) with 5 μM FURA2/AM, 1 mM probenecid and 0.02 mg/ml bovine serum albumin at 37°C for 30 min. After loading the dye, the cells were rinsed in Ca^{2+}-free buffer, containing 1 mM probenecid, and resuspended at 10^6 cells/ml in this medium. Cells were subsequently kept in the dark on ice (except when used) until the completion of the assay (routinely 4–5 h). Prior to measuring fluorescence, cells were incubated either with vehicle or varying concentrations of the muscarinic receptor antagonists, atropine or pirenzepine, at 37°C for 15 min. A final concentration of 1.8 mM $CaCl_2$ was added to the cells 5 min prior to recording traces. Fluorescence measurements were made at 37°C in a quartz microcuvette with continuous stirring at excitation wavelengths of 340 and 380 nm and an emission wavelength of 510 nm using a Perkin Elmer LS50B fluorescence spectrophotometer. For each trace, a maximum and minimum fluorescence range was determined using

60 mg/ml digitonin and 10 mM EGTA, respectively. Data were collected using FLWinLab software provided by the equipment manufacturer and free Ca^{2+} concentrations were calculated off line according to the method of Grynkiewicz et al. (1985) using a K_D value of Ca^{2+}-Fura 2 of 225 nM. Concentration–response curves to the agonists in the absence or presence of antagonist were constructed using the peak Ca^{2+} response obtained at each concentration of agonist.

2.4. Equilibrium competition binding experiments

CHO cells ($\sim 10^5$ cells per assay tube in a total volume of 1 ml) were incubated with 0.2 nM [^{3}H]*N*-methylscopolamine in the absence or presence of atropine (0.1 nM–2 μM) or pirenzepine (0.2 nM–5 μM) for 1 h at 37°C. Non-specific binding was defined using 10 μM atropine. Incubation was terminated by filtration through Whatman GF/C filters, positioned on a Brandell Cell Harvester. Filters were washed three times with 4 ml aliquots of ice-cold saline and dried before radioactivity (disintegrations per minute) was measured using liquid scintillation counting. Saturation binding parameters for [^{3}H]*N*-methylscopolamine under these conditions have been determined previously (Christopoulos et al., 1998).

2.5. Association kinetic experiments

The initial association rate of [^{3}H]*N*-methylscopolamine at the muscarinic M_1 receptor was also studied in intact CHO cells that had been pretreated with vehicle or with equivalent concentrations (with respect to receptor occupancy) of either atropine or pirenzepine, prior to extensive washout, in order to obtain an indirect measure of the unlabelled antagonists' relative rates of dissociation. Briefly, parallel groups of CHO cells were incubated with vehicle, 30 nM atropine or 2 μM pirenzepine for 30 min at 37°C in HEPES buffer. Subsequently, ice-cold buffer was added to the tubes, and the cells were centrifuged for 3 min at $300 \times g$. The resulting pellet was re-suspended in ice-cold buffer and the procedure was repeated twice prior to a final pellet re-suspension. Cells ($\sim 10^5$ cells per assay tube in a total volume of 1 ml) were subsequently incubated with 0.2 nM [^{3}H]*N*-methylscopolamine, the latter added at various times ranging from 30 s to 20 min, at 25°C before termination by vacuum filtration. Non-specific binding was defined as above.

2.6. Theoretical simulations and Monte Carlo procedures

A dynamic model of a transient response system (see Section 3) was constructed using the program Stella 5.1.1 (HPS, Hanover, NH, USA) and the resulting differential equations were executed using the program Madonna 6.0 (Macey and Oster, UCI Berkley, CA, USA). Simulated responses, characterized by a rapid peak phase followed by a sustained plateau component, were analyzed in the same fashion as the experimental Ca^{2+} data in order to construct concentration–response curves to a theoretical agonist in the absence or presence of varying concentrations of a theoretical antagonist. Agonist $p\mathrm{EC}_{50}$ and ''$p\mathrm{EC}_{25\%}$'' estimates from the theoretical curves in the absence or presence of antagonist (see Section 2.7) were then replicated 250 times with the addition of random error using a Monte Carlo procedure (Christopoulos, 1998) and the data were then analyzed to derive theoretical antagonist potency estimates, as described below.

2.7. Data analysis

Individual agonist concentration–response curves, in the absence and presence of antagonist, were fitted via nonlinear regression to the following four-parameter logistic function, using PRISM 2.01 (GraphPad Software, San Diego, CA):

$$E = \mathrm{Basal} + \frac{E_{\max} - \mathrm{Basal}}{1 + 10^{(\mathrm{LogEC}_{50} - \mathrm{Log}[A])^{n_H}}} \quad (1)$$

where E denotes effect, $\mathrm{Log}[A]$ the logarithm of the concentration of agonist, n_H the midpoint slope, LogEC_{50} the logarithm of the midpoint location parameter, and $E_{\max}$ and Basal the upper and lower asymptotes, respectively.

Antagonist potency estimates were determined using two approaches. The first represents the standard method of comparing agonist EC_{50} values obtained in the absence or presence of antagonist. Thus, the EC_{50} values derived from all agonist concentration–response curves via nonlinear regression were fitted according to the following equation (Lew and Angus, 1995):

$$p\mathrm{EC}_{50} = -\log\left([B]^s + 10^{-\mathrm{p}K}\right) - \log c \quad (2)$$

where $p\mathrm{EC}_{50}$ denotes the negative logarithm of the EC_{50}, $[B]$ denotes antagonist concentration, $\mathrm{p}K$ and $\log c$ are fitting constants, and s is equivalent to the Schild (Arunlakshana and Schild, 1959) slope factor. In the above equation, if s is not significantly different from unity, then it is constrained as such and the resulting $\mathrm{p}K$ value is equivalent to the $\mathrm{p}K_B$. Otherwise, a $p\mathrm{A}_2$ value may be determined via the relationship $p\mathrm{A}_2 = \mathrm{p}K/\mathrm{s}$. The parameter, $\log c$, equals the logarithm of the ratio of control curve EC_{50} to the K_B. Because the present study focused on potential non-equilibrium conditions, where agonist concentration–response curves can display varying maximal responses in the presence of antagonist, an alternative approach to determine antagonist potency was undertaken for comparison with the standard approach. In this latter instance, equieffective agonist concentrations (not necessarily corresponding to the EC_{50} concentration) were determined from all curves and assigned as the dependent variable in Eq. 2. This was necessary because a compari-

son of EC_{50} values under conditions of varying maximal responses violates the null-method approach of the traditional methods, which assume that the EC_{50} values being compared represent equieffective concentrations. The level representing the 25% maximal response of the control agonist curve was chosen as the reference point for the determination of equieffective agonist concentrations (''$pEC_{25\%}$'') for each family of agonist curves obtained in the presence of antagonist.

Competition binding isotherms were analyzed via nonlinear regression using PRISM in order to derive estimates of the Hill slope factor and the IC_{50} (midpoint location/potency parameter). Assuming simple competition, the data were re-fitted according to both one- and two-site mass-action binding models and the better model was determined by an extra-sum-of-squares test using PRISM. IC_{50} values were converted to K_I values (competitor–receptor dissociation equilibrium constant) according to the following equation (Cheng and Prusoff, 1973):

$$K_I = \frac{IC_{50}}{1 + ([D]/K_D)} \quad (3)$$

where $[D]$ and K_D denote the concentration and dissociation constant, respectively, of the radioligand. For the association kinetic experiments, data were fitted to the following equation for monoexponential association, in order to derive the initial, apparent association rate constant (k_{app}):

$$Y = Y_{max}(1 - e^{k_{app}t}) \quad (4)$$

where Y_{max} denotes the apparent maximal plateau of association and t denotes time.

Data shown are the mean ± S.E.M. Comparisons between means were performed by unpaired t tests, or one-way analysis of variance (ANOVA), as appropriate. Unless otherwise stated, values of $P < 0.05$ were taken as significant.

3. Results

3.1. Agonist-mediated Ca^{2+} mobilization

Activation of the muscarinic M_1 receptor by either carbachol or xanomeline resulted in a concentration-dependent increase in the intracellular levels of free Ca^{2+} (Fig. 1). The insets to the figure show typical responses to a

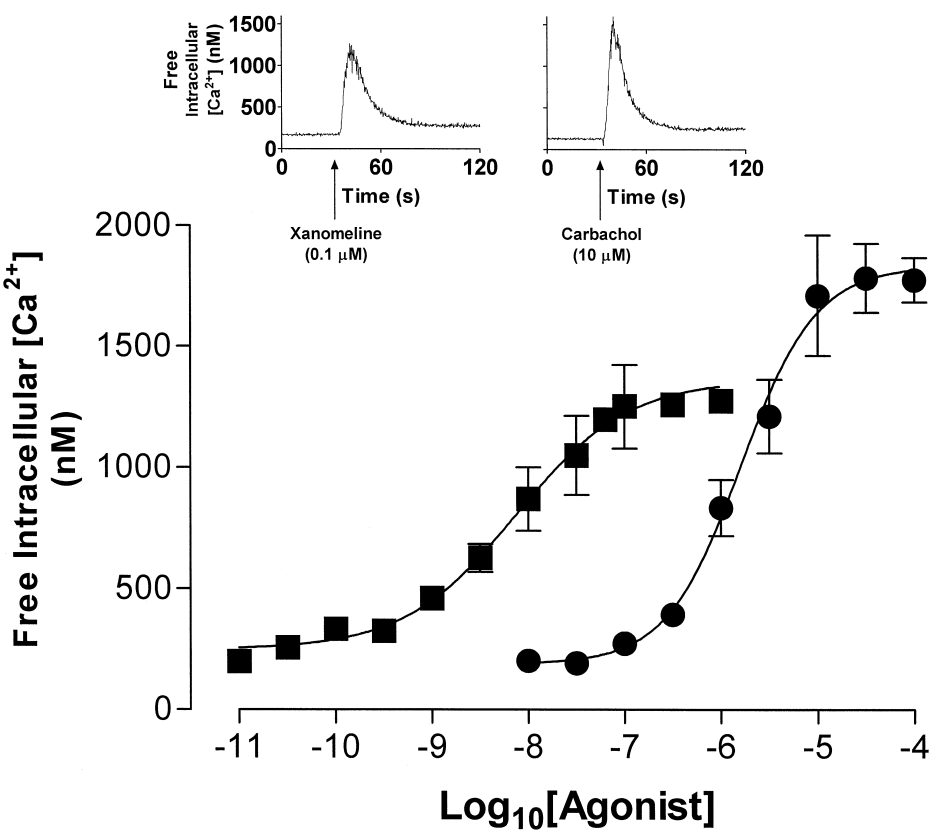

Fig. 1. Concentration–response relationships for muscarinic M_1 receptor-mediated intracellular Ca^{2+} mobilization by the agonists carbachol (●) and xanomeline (■) in CHO cells. Symbols represent the mean ± S.E.M. of 8–10 experiments. Insets: Representative recording of a Ca^{2+} response to 0.1 μM xanomeline, left, and 10 μM carbachol, right.

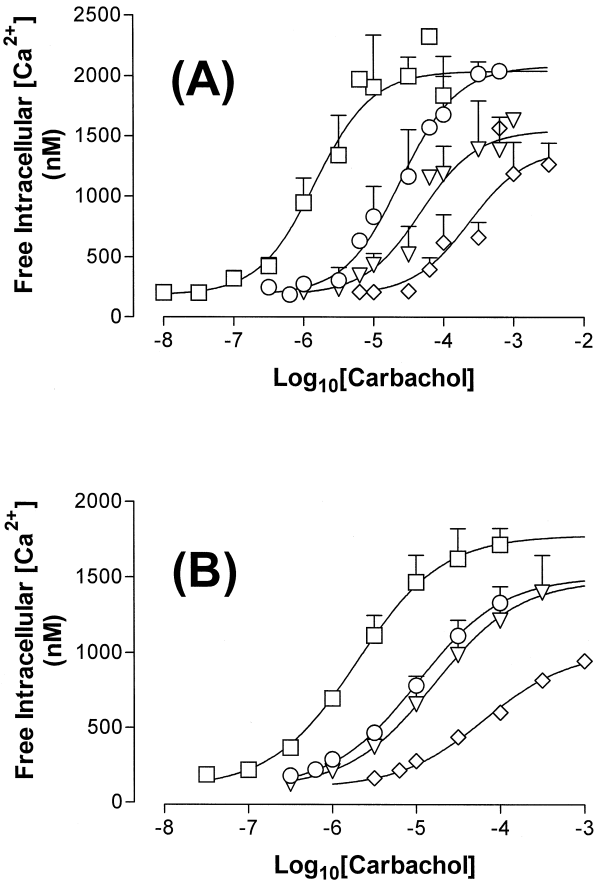

Fig. 2. Inhibition of carbachol-mediated intracellular Ca^{2+} mobilization by (A) atropine and (B) pirenzepine in CHO cells. Effects of carbachol in the absence (□) or presence of (A) 10 (○), 30 (▽) or 100 (◇) nM atropine or (B) 50 (○), 150 (▽) or 500 (◇) nM pirenzepine. Cells were equilibrated with antagonist for 15 min at 37°C before the addition of agonist or vehicle control. Symbols represent the mean + S.E.M. of 3–5 experiments.

single concentration of either carbachol or xanomeline, where it can be seen that the muscarinic M_1 receptor-mediated Ca^{2+} response consists of two phases, a rapid peak response followed by a gradual decline to a plateau value. By using the peak response obtained at each concentration of agonist, the concentration–response relationship for carbachol- and xanomeline-mediated Ca^{2+} mobilization could be determined (Fig. 1). Nonlinear regression analysis according to Eq.(1) yielded the following logistic parameters: carbachol ($n = 10$); $E_{max} = 1833 \pm 118$ nM, $pEC_{50} = 5.79 \pm 0.13$, $n_H = 1.11 \pm 0.35$, Basal $= 188 \pm 113$ nM; xanomeline ($n = 8$); $E_{max} = 1360 \pm 190$ nM, $pEC_{50} = 8.13 \pm 0.26$, $n_H = 0.74 \pm 0.31$, Basal $= 247 \pm 92$ nM. Although xanomeline was significantly more potent than carbachol ($P < 0.05$) in stimulating intracellular Ca^{2+} mobilization, it behaved as a partial agonist relative to the latter agent, having an intrinsic activity of approximately 0.74 times that of carbachol (Fig. 1). Thus, xanomeline cannot stimulate a maximal Ca^{2+} response even at full receptor occupancy.

3.2. Pharmacological analysis of the antagonism by atropine or pirenzepine of carbachol or xanomeline-mediated Ca^{2+} responses

The presence of increasing concentrations of either atropine or pirenzepine resulted in progressive degrees of dextral shift of the carbachol (Fig. 2) or xanomeline (Fig. 3) concentration–response curves for muscarinic M_1 receptor-mediated Ca^{2+} mobilization. However, in no instance did the antagonism appear consistent with simple, surmountable competition. As the antagonist concentration was increased, the agonist concentration–response curves displayed different degrees of reduction in maximal response. Specifically, the degrees of depression of agonist concentration–response curve maxima observed in the presence of the highest concentration of antagonist, relative to the absence of antagonist, were as follows: carbachol/atropine, 68%; carbachol/pirenzepine, 57%; xanomeline/atropine, 57%; xanomeline/pirenzepine, 39%. Interestingly, varying patterns of inhibition could be

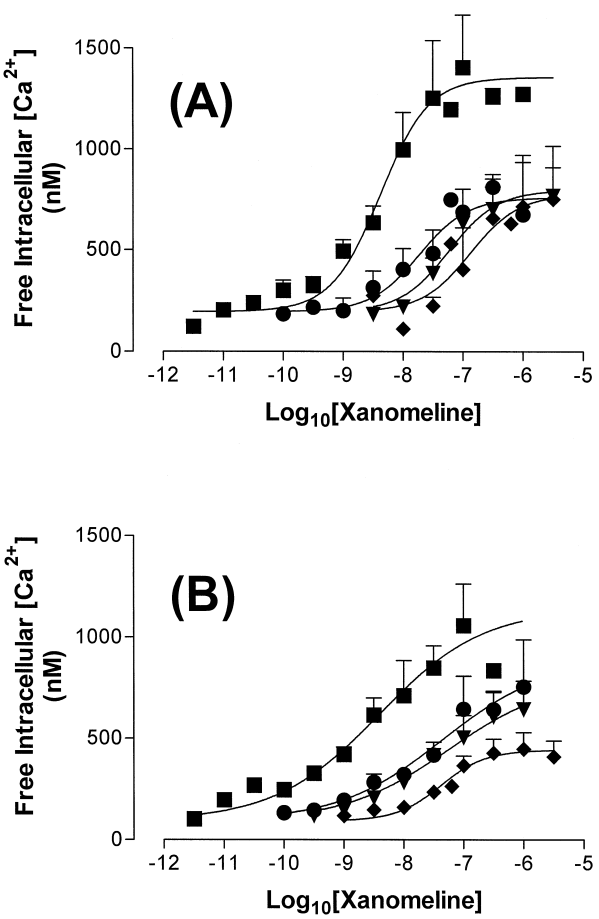

Fig. 3. Inhibition of xanomeline-mediated intracellular Ca^{2+} mobilization by (A) atropine and (B) pirenzepine in CHO cells. Effects of xanomeline in the absence (■) or presence of (A) 10 (●), 30 (▼) or 100 (◆) nM atropine or (B) 50 (●), 150 (▼) or 500 (◆) nM pirenzepine. Symbols represent the mean + S.E.M. of 3 experiments. Other details as for Fig. 2.

discerned, including an apparent *saturable* depression of agonist maximal response (Fig. 3A).

Although the concentration–response data did not conform to the minimum criteria for simple, surmountable, competitive antagonism, the relationship between the agonist pEC_{50} values and the concentrations of each antagonist was utilized, without prejudice to mechanism, to obtain pA_2 estimates as approximate measures of relative antagonist potencies. These results, derived via fitting the data to Eq. (2) are shown in Table 1.

3.3. Determination of antagonist potency under equilibrium conditions using radioligand competition binding

In order to obtain estimates of antagonist dissociation constants that are not confounded by kinetic artifacts, competition binding experiments were undertaken using the antagonist, [^{3}H]*N*-methylscopolamine as the radioligand. Fig. 4 shows the results of these experiments, conducted on intact CHO cells using the same buffer as the functional assays, where it can be seen that both atropine and pirenzepine were able to completely inhibit the binding of 0.2 nM [^{3}H]*N*-methylscopolamine in a concentration-dependent manner. Nonlinear regression analysis of the data revealed that in each instance, a one-site binding model provided an adequate fit. For atropine, the pK_I value was estimated as 8.59 ± 0.15 and the Hill slope was 0.93 ± 0.12 ($n = 4$). For pirenzepine, the pK_I was 7.63 ± 0.16 and the Hill slope was 0.99 ± 0.07 ($n = 5$).

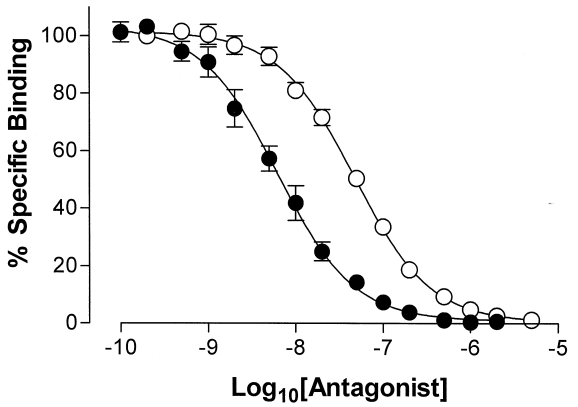

Fig. 4. Inhibition of 0.2 nM [^{3}H]*N*-methylscopolamine binding by atropine (●) or pirenzepine (○) in CHO cells. Incubation was for 1 h at 37°C. Nonspecific binding was defined using 10 μM atropine. Symbols represent the mean ± S.E.M. of 4–5 experiments conducted in triplicate.

3.4. Comparison of relative rates of antagonist dissociation

If the apparent insurmountability of antagonism observed in the present study was, in fact, due to an artifact related to slow antagonist kinetics, then the degree of depression would be expected to be inversely related to the dissociation rate of the antagonist. Since atropine is no longer commercially available in radiolabelled form, an indirect approach was utilized to obtain a relative measure of its dissociation rate in comparison to pirenzepine. Initially, cells were pretreated with equivalent concentrations (with respect to receptor occupancy) of atropine or pirenzepine (approximately $\times 30 K_I$) for 30 min at 37°C, at which time equilibrium was achieved (not shown). Subsequently, the unbound antagonists were removed by extensive washout on ice and the association rate of [^{3}H]*N*-methylscopolamine was monitored over time at 25°C. It can be seen from the representative experimental results in Fig. 5 that the radioligand displayed a markedly slower initial rate of association in the cells that had been pretreated with pirenzepine when compared to atropine-pretreated cells. This implies that pirenzepine must dissociate from the receptor at a slower rate than atropine, even though the latter has higher affinity. A fit of the data to Eq. (4) showed that both atropine and pirenzepine slowed the initial association rate of [^{3}H]*N*-methylscopolamine

Table 1
Semiquantitative estimates of antagonist potency for the inhibition of muscarinic M_1 receptor-mediated mobilization of intracellular Ca^{2+} in CHO cells. Experiments were conducted at 37°C in real time using a spectrofluorometric assay

Agonist	Antagonist	pEC_{50} [a]		$pEC_{25\%}$ [b]		d.f. [e]
		pA_2 [c]	Slope [d]	pA_2 [c]	Slope [d]	
Carbachol	Atropine	9.12 ± 0.21	1.09 ± 0.18	8.64 ± 0.15	1.09 ± 0.18	11
Xanomeline		8.93 ± 0.35	1.10 ± 0.57	8.73 ± 0.18	1.09 ± 0.25	13
Carbachol	Pirenzepine	7.83 ± 0.42	0.86 ± 0.28	7.67 ± 0.25	0.89 ± 0.18	6
Xanomeline		7.76 ± 0.47	0.71 ± 0.48	7.49 ± 0.21	0.82 ± 0.25	6

[a] Antagonist parameter estimates were derived by nonlinear regression analysis of agonist pEC_{50} values, obtained in the presence or absence of increasing concentrations of antagonist, according to Eq. (2) of Section 2.

[b] Antagonist parameter estimates were derived by nonlinear regression analysis of equieffective agonist concentrations, corresponding to 25% maximal control agonist response, obtained in the presence or absence of increasing concentrations of antagonist, according to Eq. (2) of Section 2.

[c] Negative logarithm of the apparent antagonist potency, derived using Eq. (2) of Section 2.

[d] Schild slope factor estimated from Eq. (2) of Section 2. All values were not significantly different ($P > 0.05$) from unity.

[e] Degrees of freedom.

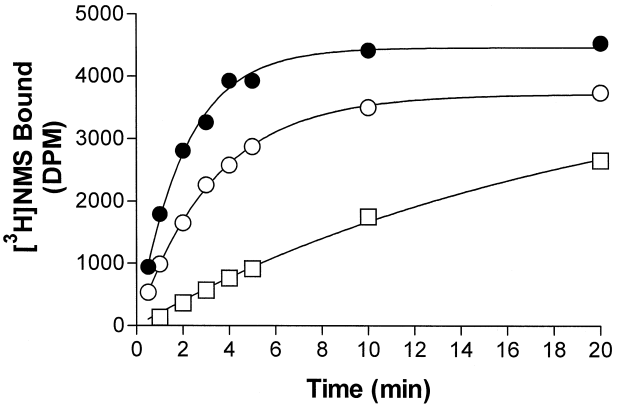

Fig. 5. Association of 0.2 nM [^{3}H]*N*-methylscopolamine in CHO cells that had been pretreated with either vehicle (●), 30 nM atropine (○) or 2 μM pirenzepine (□) at 37° C for 30 min prior to extensive washout on ice. Curves are representative of a single experiment conducted in triplicate at 25°C.

(vehicle-pretreated, 0.47 ± 0.02 min^{11}; atropine-pretreated, 0.29 ± 0.03 min^{11}; pirenzepine-pretreated, 0.04 ± 0.01 min^{11}; $P < 0.001$ by one-way ANOVA, $n = 3$ each group). Thus, pirenzepine has an approximately 8-fold slower rate of dissociation from the muscarinic M_1 receptor than atropine under these conditions. This observation is consistent with the more pronounced maximal depression of agonist concentration–response curves observed when pirenzepine is used as the antagonist, rather than atropine (Figs. 2 and 3).

3.5. Development of a dynamic model of transient response kinetics

Although an analysis of pEC_{50} values was undertaken to obtain approximate, empirical, estimates of antagonist potency (Table 1), it is obvious that the application of a standard equilibrium-based formulation to a non-equilibrium situation would be expected to yield values that can deviate from those obtained under true equilibrium conditions. In situations such as the present case where a non-equilibrium condition appears unavoidable, it is desirable to obtain a measure of the reliability of antagonist potency estimates derived using the standard methods. Thus, a dynamic model was constructed in an attempt to account for the present observations and to assess the reliability of antagonist potency estimates obtained under these conditions.

The model is outlined in Fig. 6 and the description of the relevant rate constants is shown in the legend to the figure. A salient feature of the model is that the rate of transition (k_3) of response-generating species (AR) to a form no longer capable of generating the same response (AR_D) is determined not only by a ''desensitization'' rate constant (''desens. rate''; Fig. 6), but also by the response itself. This distinguishes the model from previous, occupancy-based dynamic schemes (e.g., Kukkonen et al., 1998), as it accounts for the ability of post-receptor events to influence the rate of response transience, ''fade'' or ''shut-off''. In this example, response is modeled as a hyperbolic function of [AR], but steep or shallow concentration–response curves can also be simulated by allowing the logistic slope factor, n (Fig. 6), to have values other than 1. In addition, the parameter K_E is included as an efficacy term that accounts for the sensitivity of stimulus–response coupling (Kenakin and Beek, 1980; Black and Leff, 1983).

The model gives responses that peak and then decline, with the time-course governed by the parameters k_3 and k_4. Fig. 7 shows a series of simulated agonist concentration–response curves ($pK_A = 7$; $K_E = 0.1$) obtained in the absence or presence of a competitive antagonist ($pK_B = 9$). Values for the individual rate constants are shown in the legend to the figure. The peak response level to each concentration of agonist was utilized to construct the

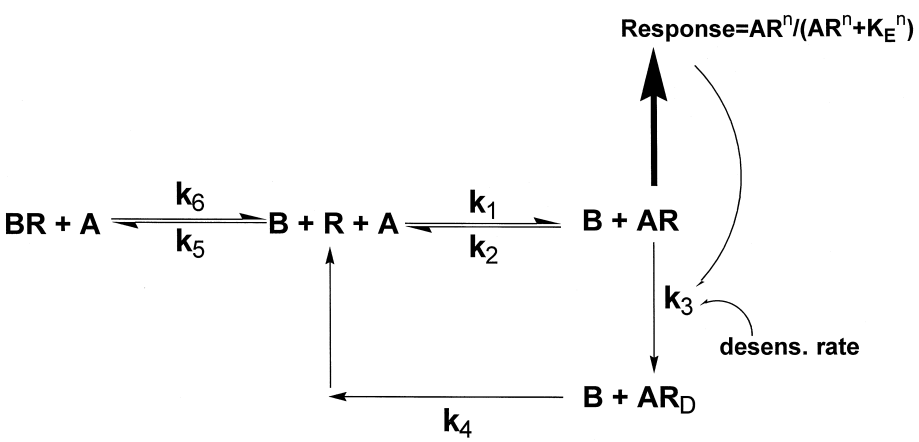

Fig. 6. A dynamic model of a transient response system. A, B and R denote the free agonist, antagonist and receptor species, respectively. Parameters k_1 and k_5 denote agonist and antagonist association rate constants, respectively, whereas k_2 and k_6 denote agonist and antagonist dissociation rate constants, respectively. The response is determined by the rate of formation of AR species, and is a logistic function of AR, where K_E denotes the efficiency of response generation and n is a logistic slope factor. Response fade (transition to AR_D species) is determined by k_3, the latter constant being the product of the desens. rate constant and the response. Resensitization is determined by the rate constant, k_4.

curves. Furthermore, it was assumed that the antagonist had pre-equilibrated with the receptor pool prior to the addition of agonist. It can be seen from Fig. 7 that increasing concentrations of antagonist result in a saturable depression of agonist concentration–response curve maximum. This is akin to what was observed experimentally for the interaction between atropine and xanomeline (Fig. 3A), and the saturability cannot be accounted for by previously described kinetic artifacts related to hemi-equilibrium states (see Section 4). By decreasing the rate of antagonist dissociation (k_6) and/or decreasing the agonist efficacy (K_E), the depression may be exacerbated to the point of appearing completely insurmountable (not shown). Conversely, increased antagonist dissociation and/or agonist efficacy yield an antagonistic pattern compatible with surmountable competition.

Also shown in Fig. 7 are the locations of the EC_{50} response levels for each agonist concentration–response curve, where it is apparent that they correspond to concentrations of agonist that are not equieffective. Since the location and nature of the agonist concentration–response curve is affected by the response transience and by the antagonist kinetics, the pA_2 value obtained from a normal Schild-type analysis (Eq. (2) using pEC_{50} values) may not accurately reflect the antagonist pK_B. This can be seen in Fig. 8A where 250 pEC_{50} values, obtained in the absence or presence of antagonist, were simulated by Monte Carlo analysis and subsequently analyzed according to Eq. (2). The Monte Carlo procedure consisted of the addition of a random number, taken from a Gaussian population with a mean of 0 and a standard deviation of 0.25, to the true pEC_{50} value derived from the modeling. The true antagonist pA_2 value of 9 is associated with a very large spread of values (Fig. 8A). In contrast, a similar analysis using curve locations from a constant level of response ($E/E_{max} = 0.25$ in Fig. 7) gave a tighter estimate of pA_2 than using pEC_{50} values (Fig. 8B).

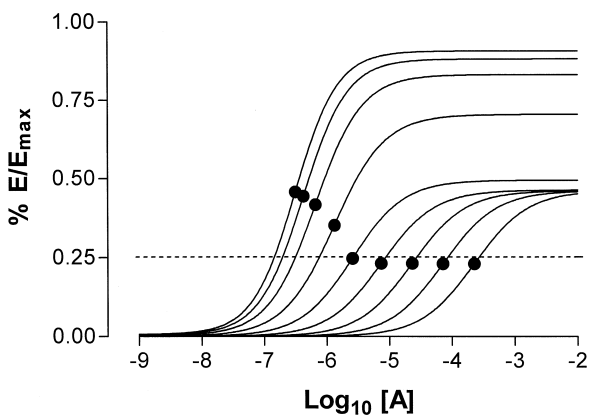

Fig. 7. Simulated concentration–response curves for an agonist/antagonist pair according to the dynamic model in Fig. 6 and the following rate constants: $k_1 = 10^6$, $k_2 = 0.1$, $k_4 = 0.1$, $k_5 = 10^9$, $k_6 = 1$, $K_E = 0.1$, desens. rate = 1 and k_3 = desens. rate × response. Antagonist concentration units range from 3×10^{-10} to 10^{-6} in increments of 0.5 log. units. Curve locations, as defined by the EC_{50}, are shown as solid circles. Dotted line represents arbitrarily chosen response level for the determination of equieffective agonist concentrations in order to estimate antagonist potency (see Fig. 8).

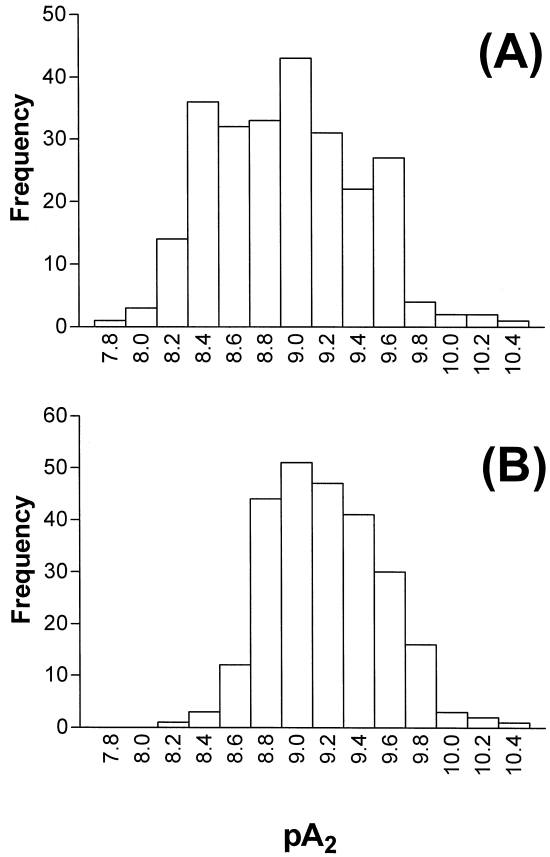

Fig. 8. Frequency distributions of pA_2 values determined via nonlinear regression analysis of 250 simulated datasets according to the model depicted in Figs. 6 and 7. Values in (A) were determined by regression analysis of pEC_{50} values, whereas values in (B) were determined by regression analysis of equieffective agonist concentrations (corresponding to the 25% maximal response level of the control agonist curve; dotted line in Fig. 7) in the absence and presence of antagonist.

The experimental data in Figs. 2 and 3 were re-analyzed according to the above modification, with the 25% response level of the control agonist curve being utilized as the reference point for the determination of equieffective agonist concentrations (''$pEC_{25\%}$'' approach). The resulting antagonist parameter estimates, via analysis according to Eq. (2), are also shown in Table 1. Although not very different from those obtained using the pEC_{50} values, the latter estimates are associated with smaller errors, as the results of the above simulations implied, and are in excellent agreement with the values obtained at equilibrium in the competition binding assays.

4. Discussion

The muscarinic receptor agonists, carbachol and xanomeline, both elicited rapid mobilization of intra-

cellular Ca^{2+} that was inhibited by the antagonists atropine and pirenzepine, but the antagonism did not display the classical hallmarks of competitive, reversible antagonism (namely, a surmountable rightward shift of the agonist concentration–response curve). Instead, the rightward shift was accompanied by a saturable depression of the agonist maximum response, with the amount of depression varying with each combination of agonist and antagonist. By contrast, the equilibrium inhibition binding experiments found no evidence for deviation of the interaction between the radioligand and either atropine or pirenzepine from simple competition. Furthermore, the estimates of the antagonists' dissociation constants were in very good agreement with previously reported values (Mitchelson, 1988; Caulfield, 1993). Each antagonist was able to significantly slow the rate of association of [^{3}H]*N*-methylscopolamine with the receptor, with atropine slowing the association about 8 times more than pirenzepine. The results of our numerical dynamic simulations predict that where a competitive reversible antagonist slows the rate of response onset in a system with transient agonist response kinetics there may be a saturable depression of the agonist maximum response. Because the Ca^{2+} responses that we measured are intrinsically transient we can explain the experimental data on that basis. The functional data did not match the classical predictions for a competitive reversible interaction because the conditions of the interaction did not meet the classical assumption of equilibrium.

In practice, there are at least three broad situations that can invalidate the assumption of equilibrium conditions in the characterization of an antagonistic effect. These are: (i) the time course of the experiment is inadequate; (ii) rapid receptor desensitization, internalization or other form of uncoupling and (iii) rapid response fade in spite of sustained receptor activation, that is, as a consequence of post-receptor events. The first case is important when an antagonist dissociates so slowly from the receptor over the time course of the experiment that it behaves as if it were truly irreversible. This represents one of the most common (and best-studied) examples of insurmountable antagonism, and methods have been developed that allow for the calculation of dissociation constants under these conditions for both agonists and antagonists (Furchgott, 1966; Paton and Waud, 1967; Kenakin, 1997; Kenakin and Cook, 1980). A special case of this phenomenon has been termed the ''hemi-'' or ''quasi-equilibrium'' by Paton et al. (Paton and Rang, 1966; Paton and Waud, 1967). The hemi-equilibrium state, as originally described, occurs when a response to an agonist, in the presence of a fixed concentration of a pre-equilibrated antagonist, is a result of an *equilibrium* interaction between the agonist and the free receptor pool *with no concomitant perturbation* of the pre-existing antagonist equilibrium (Paton and Rang, 1966). Obviously, a readjustment of receptor occupancy must eventually ensue (that is, a non-equilibrium condition will be created), but this is considered to occur *after* the response of interest has been measured. To fulfill the criteria of a strict hemi-equilibrium state, therefore, an agonist must first rapidly equilibrate with the free receptor pool and then evoke a response that is measured before *any* readjustment of antagonist-receptor occupancy occurs. Often, these assumptions are overlooked when the phenomenon is described in the literature. In particular, the hemi-equilibrium *cannot* account for the observation of a saturable depression of the agonist concentration–response relationship in the presence of increasing antagonist concentrations (Fig. 3A, Fig. 7); instead the maximal response to a given partial agonist under hemi-equilibrium conditions should be modified by a constant factor proportional to $K_B/(K_B + [B])$, where K_B and $[B]$ refer to the equilibrium dissociation constant and concentration of antagonist, respectively. Therefore, although often quoted in the literature as a possible mechanism in the description of insurmountable antagonism due to kinetic artifacts, the strict hemi-equilibrium state probably does not apply to many of them. This would have a profound effect on the quantitative estimation of antagonist potency parameters according to the equations of classical receptor theory that assume equilibrium between agonist, antagonist and receptor. Nevertheless, a relationship between antagonist dissociation rate and degree of depression of agonist concentration–response curve maximum is predicted in situations related to kinetic artifacts, irrespective of the existence of a true hemi-equilibrium. In this context, it is noteworthy that the degree of depression of either carbachol's or xanomeline's concentration–response curve maximal asymptote appeared more pronounced when pirenzepine was utilized as the antagonist (Figs. 2B, 3B), this latter agent possessing a slower apparent dissociation rate than atropine (Fig. 5).

The effects on the quantification of antagonist potency during the operation of the other two conditions that invalidate the equilibrium assumption, that is, desensitization and/or rapid response fade due to a post-receptor mechanism, have not been studied in as great a detail. However, they too can yield results that may often be (incorrectly) interpreted in terms of a hemi-equilibrium state. The model depicted in Fig. 6 adequately describes this situation and predicts that the effect of receptor desensitization and/or post-receptor rapid response fade would be to exacerbate *both* the apparent insurmountability of antagonism and the lack of sufficient agonist equilibration during the time-scale of response measurement in a manner related to antagonist dissociation kinetics and agonist efficacy. In accordance with this prediction, the most severe case of insurmountable antagonism was observed for the combination of pirenzepine (slower antagonist) and xanomeline (least efficacious agonist), whereas the least severe case appeared to be for the combination of atropine (faster antagonist) and carbachol (more efficacious agonist). It should be noted, however, that the model described in our study is one of several possible dynamic mecha-

nisms that may adequately account for the experimental findings. It was chosen as the simplest scheme allowing for both agonist-mediated receptor desensitization and output-mediated response shut-off. For example, this model could accommodate a rapid decline in peak Ca^{2+} levels as a result of the operation of cellular Ca^{2+} pumping, rather than due to agonist-mediated desensitization. In any case, the results of the dynamic simulations appear to indicate that *any* mechanism leading to rapid and transient responses can also lead to the appearance of insurmountable antagonism. Furthermore, this type of non-equilibrium situation may result in the phenomenon of saturable depression of an agonist concentration–response curve in conjunction with dextral curve shifts (Fig. 7). Kukkonen et al. (1997, 1998) have recently presented similar data while evaluating the hypothesis that insurmountability of antagonism by agents that appear competitive in other assays is directly related to the kinetics of antagonist dissociation.

Interestingly, the phenomenon of saturable depression of agonist concentration–response curves in the presence of antagonist has been previously reported in the literature, particularly with regard to the interaction between angiotensin II and a series of peptide and non-peptide antagonists (Liu et al., 1992; Criscione et al., 1993; Robertson et al., 1994; Hara et al., 1995). Although kinetic artifacts have been considered in some studies (e.g., Hara et al., 1995), others have presented models based on specific equilibrium mechanisms to account for the data. For instance, Liu et al. (1992) presented a model whereby antagonism occurred in conjunction with antagonist-induced steady-state internalization. Robertson et al. (1994) have explained similar observations by postulating antagonist-induced desensitization with a two-state model of receptor action. It is possible that all these observations may be reconciled with a transient response system that fades prior to adequate agonist equilibration time.

An important consideration of all the situations described above is the impact on the estimation of antagonist potency parameters. By assuming an equilibrium reaction, estimates may be derived that relate the observations to the equilibrium occupancy of the receptor by the antagonist in terms of the latter's concentration and its equilibrium dissociation constant. However, these estimates must also account for the deviations of the experimental data from simple, surmountable competition and thus require the construction of increasingly complex equilibrium formalisms. If the data are truly due to a non-equilibrium situation, then all equilibrium-based analytical methods, irrespective of their elegance and/or complexity, can only be expected to provide, at best, a semi-quantitative, ad hoc measure of antagonist potency. With this in mind, we chose to utilize the simplest equilibrium formulation for expressing antagonist potency, namely, Schild's pA_X scale (Schild, 1949) and to test how well it may be utilized to derive semi-quantitative antagonist potency estimates. From the Monte Carlo simulations (Fig. 8), it can be seen that reasonable estimates of the equilibrium antagonist potency may be derived by a comparison of equieffective agonist concentration in the absence and presence of antagonist, provided that the degree of maximal depression is not too pronounced. Indiscriminate comparison of EC_{50} concentrations should not be attempted. Where the depression of maximal asymptote of the agonist concentration–response curve does not appear to saturate, the limiting case would be indistinguishable from the hemi-equilibrium situation, in which case the standard methods for analyzing irreversible antagonism may be utilized (Kenakin and Cook, 1980). However, the same cannot be said for the estimation of agonist affinity from such data, as the response may be measured when the agonist is not at equilibrium. This latter situation may be unavoidable due to the transient nature of the response and does not appear to have been considered in the past when transient response systems and slowly dissociating antagonists have been utilized to extract agonist affinity estimates.

Obviously, the semi-quantitative approach outlined in this study is not intended to represent the ideal means for obtaining accurate measures of antagonist (or agonist) potency. Within the framework of the dynamic model in Fig. 6, the individual rate constants for agonist and antagonist binding, as well as response ''turn-on'' and ''shut-off'' must be determined. At the moment, this is not possible for many systems and even when it is, it is often cumbersome to do so if the aim of the study is to obtain some sort of relative measurement or rank order of potency. It is with this latter situation in mind that the current approach may prove most useful. A comparison of the ''optimized'' antagonist potency estimates ($pEC_{25\%}$ column, Table 1) with the data derived in the equilibrium binding assays shows excellent agreement, and bypasses the need to postulate additional equilibrium mechanisms to account for the interaction. Where the data are consistent with pure insurmountability and no change in agonist curve location, the method of Furchgott (1966) may be utilized to determine an approximate estimate of antagonist potency (Kenakin and Cook, 1980). Where a saturable depression of agonist concentration–response curve maximum occurs in the presence of antagonist, it is suggested that the current method may prove suitable.

In conclusion, the present study has demonstrated that an apparent insurmountability of antagonism may be observed for the interaction between competitive and reversible agonist–antagonist pairs when the agonist response is affected by a rapid fade phenomenon. A minor modification of standard Schild-type analysis may be utilized to derive reasonable estimates of antagonist potency, thus bypassing the need to postulate complex equilibrium reaction schemes in accounting for and analyzing the data. The application of this approach to the interaction between the muscarinic agonists carbachol or xanomeline and the antagonists atropine or pirenzepine yielded good agreement with antagonist potency estimates determined from

equilibrium binding studies. It should also be noted that, in vivo, non-equilibrium steady-states are more often the rule, rather than the exception, and further studies of the dynamic consequences of agonist–antagonist interactions appear warranted.

Acknowledgements

The authors are grateful to Miss Negar Vahdat-Hagh for excellent technical assistance. This work was supported by National Institutes of Health Grant No. NS25743.

References

Arunlakshana, O., Schild, H.O., 1959. Some quantitative uses of drug antagonists. Br. J. Pharmacol. 14, 48–57.

Black, J.W., Leff, P., 1983. Operational models of pharmacological agonism. Proc. R. Soc. (London) B 220, 141–162.

Bond, R.A., Ornstein, A.G., Clarke, D.E., 1989. Unsurmountable antagonism to 5-hydroxytryptamine in rat kidney results from pseudoirreversible inhibition rather than multiple receptors or allosteric receptor modulation. J. Pharmacol. Exp. Ther. 249, 401–410.

Boselli, C., Kenakin, T.P., 1990. Promiscuous or heterogeneous muscarinic receptors in rat atria? II. Antagonism of responses to carbachol by pirenzepine. Eur. J. Pharmacol. 191, 49–57.

Caulfield, M.P., 1993. Muscarinic receptors — characterization, coupling and function. Pharmacol. Ther. 58, 319–379.

Cheng, Y.-C., Prusoff, W.H., 1973. Relationship between the inhibition constant (K_I) and the concentration of inhibitor which causes 50 per cent inhibition (I_{50}) of an enzymatic reaction. Biochem. Pharmacol. 22, 3099–3108.

Christopoulos, A., 1998. Assessing the distribution of parameters in models of ligand–receptor interaction: to log or not to log. Trends Pharmacol. Sci. 19, 351–357.

Christopoulos, A., El-Fakahany, E.E., 1999. The qualitative and quantitative assessment of relative agonist efficacy. Biochem. Pharmacol. 58, in press.

Christopoulos, A., Pierce, T.L., Sorman, J.L., El-Fakahany, E.E., 1998. On the unique binding and activating properties of xanomeline at the M_1 muscarinic acetylcholine receptor. Mol. Pharmacol. 53, 1120–1130.

Colquhoun, D., 1998. Binding, gating, affinity and efficacy: the interpretation of structure–activity relationships for agonists and of the effects of mutating receptors. Br. J. Pharmacol. 125, 924–947.

Criscione, L., de Gasparo, M., Buhlmayer, P., Whitebread, S., Ramjoue, H.P., Wood, J., 1993. Pharmacological profile of valsartan: a potent, orally active, nonpeptide antagonist of the angiotensin II AT1-receptor subtype. Br. J. Pharmacol. 110, 761–771.

El-Fakahany, E.E., Surichamorn, W., Amrhein, C.L., Stenstrom, S., Cioffi, C.L., Richelson, E., McKinney, M., 1988. Pseudo-noncompetitive antagonism of muscarinic receptor-mediated cyclic GMP formation and phosphoinositide hydrolysis by pirenzepine. J. Pharmacol. Exp. Ther. 247, 934–940.

Furchgott, R.F., 1966. The use of β-haloalkylamines in the differentiation of receptors and in the determination of dissociation constants of receptor–agonist complexes. Adv. Drug Res. 3, 21–55.

Grynkiewicz, G., Poenie, M., Tsien, R.Y., 1985. A new generation of Ca^{2+} indicators with greatly improved fluorescence properties. J. Biol. Chem. 260, 3440–3450.

Hara, M., Kiyama, R., Nakajima, S., Kawabata, T., Kawakami, M., Ohtani, K., Itazaki, K., Fujishita, T., Fujimoto, M., 1995. Kinetic studies on the interaction of nonlabeled antagonists with the angiotensin II receptor. Eur. J. Pharmacol. 289, 267–273.

Kachur, J.F., Allbee, W.E., Gaginella, S., 1988. Antihistaminic and antimuscarinic effects of amitriptyline on guinea pig ileal electrolyte transport and muscle contractility in vitro. J. Pharmacol. Exp. Ther. 245, 455–459.

Kenakin, T.P., 1997. Pharmacologic analysis of drug-receptor interaction, 3rd edn. Lippincott–Raven Press, Philadelphia, PA.

Kenakin, T.P., Beek, D., 1980. Is prenalterol (H133/80) really a selective *beta* 1 adrenoceptor agonist? Tissue selectivity resulting from differences in stimulus–response relationships. J. Pharmacol. Exp. Ther. 213, 406–413.

Kenakin, T.P., Boselli, C., 1990. Promiscuous or heterogeneous muscarinic receptors in rat atria? I. Schild analysis with simple competitive antagonists. Eur. J. Pharmacol. 191, 39–48.

Kenakin, T.P., Cook, D.A., 1980. *N,N*-diethyl-2-(1-pyridyl)ethylamine, a partial agonist for the histamine receptor in guinea pig ileum. Can. J. Physiol. Pharmacol. 58, 1210–1307.

Kukkonen, J.P., Huifang, G., Jansson, C.C., Wurster, S., Cockroft, V., Savola, J.-M., Åkerman, K.E.O., 1997. Different apparent modes of inhibition of α_{2A}-adrenoceptor by α_2-adrenoceptor antagonists. Eur. J. Pharmacol. 335, 99–105.

Kukkonen, J.P., Näsman, J., Rinken, A., Dementjev, A., Åkerman, K.E.O., 1998. Pseudo-noncompetitive antagonism of M_1, M_3, and M_5 muscarinic receptor-mediated Ca^{2+} mobilization by muscarinic antagonists. Biochem. Biophys. Res. Commun. 243, 41–46.

Lew, M.J., Angus, J.A., 1995. Analysis of competitive agonist–antagonist interactions by nonlinear regression. Trends Pharmacol. Sci. 16, 328–337.

Liu, Y.J., Shankley, N.P., Welsh, N.J., Black, J.W., 1992. Evidence that the apparent complexity of receptor antagonism by angiotensin II analogues is due to a reversible and syntopic action. Br. J. Pharmacol. 106, 233–241.

Mitchelson, F., 1988. Muscarinic receptor differentiation. Pharmacol. Ther. 37, 357–423.

Paton, W.D.M., Rang, H.P., 1966. A kinetic approach to the mechanism of drug action. Adv. Drug Res. 3, 57–80.

Paton, W.D.M., Waud, D.R., 1967. The margin of safety of neuromuscular transmission. J. Physiol. 191, 59–90.

Robertson, M.J., Dougall, I.G., Harper, D., McKechnie, C.W., Leff, P., 1994. Agonist–antagonist interactions at angiotensin receptors: application of a two-state receptor model. Trends Pharmacol. Sci. 15, 364–369.

Schild, H.O., 1949. pAx and competitive drug antagonism. Br. J. Pharmacol. 4, 277–280.

Wotta, D.R., Parsons, A.M., Hu, J., Grande, A.W., El-Fakahany, E.E., 1998. M_1 muscarinic receptors stimulate rapid and prolonged phases of neuronal nitric oxide synthase activity: involvement of different calcium pools. J. Neurochem. 71, 487–497.